

Numerical Methods for A Quantum Energy Transport Model Arising in Scaled MOSFETs

Shohiro Sho

Graduate School of Information Science and Technology,
Osaka University
Osaka, Japan
shohiro@cas.cmc.osaka-u.ac.jp

Shinji Odanaka

Computer Assisted Science Division, Cybermedia Center,
Osaka University
Osaka, Japan
odanaka@cmc.osaka-u.ac.jp

Abstract—This paper describes numerical methods for a four-moments quantum energy transport(QET) model, which is derived by using a diffusion scaling in the quantum hydrodynamic model. Space discretization is performed by a new set of unknown variables. Numerical stability and convergence are obtained by developing an iterative solution method with a relaxation method. Numerical results in a scaled MOSFET are discussed. The QET model allows simulations of quantum confinement transport, and nonlocal and hot-carrier effects in scaled MOSFETs.

Keywords; *simulation, quantum energy transport model, MOSFET.*

I. INTRODUCTION

The performance of scaled MOSFETs relies on the quantum confinement transport, and nonlocal and hot-carrier effects in the short channels. Quantum energy transport(QET) models are required to understand such physical phenomena in scaled MOSFETs. The full QET model has been derived from the collisional Wigner-Boltzmann equations using the entropy minimization principle [1]. Numerical simulations using this model, however, have not been performed. Simplified models have been proposed as the energy transport extension of the QDD model with Fourier law closure and numerically investigated [2], [3].

In this work, we develop numerical methods for a QET model derived from a quantum hydrodynamic model. To overcome the difficulties associated with the Fourier law closure, we derive a four moments QET model. The numerical stability is achieved by discretization and an iterative solution method in terms of a new set of variables. Numerical results in a scaled MOSFET are discussed.

II. QUANTUM ENERGY TRANSPORT MODEL

The quantum hydrodynamic model has been derived from a Chapman-Enskog expansion of the Wigner-Boltzmann equation adding a collision term [4], [5]. For classical hydrodynamic simulations, the closure relation based on the four-moments of the Boltzmann equation has been proposed [6], and the four-moments ET models are discussed for simulations of thin body MOSFETs [7], [8]. In this work, a four-moments QET model is derived by using a diffusion

scaling in the four moment equations with quantum corrections to the stress tensor P_{ij} [4] and the energy density W [9], which are given by

$$P_{ij} = -nkT_n \delta_{ij} - \frac{\hbar^2}{12m} n \frac{\partial^2}{\partial x_i \partial x_j} \log n + O(\hbar^4), \quad (1)$$

and

$$W = \frac{1}{2} mnv^2 + \frac{3}{2} nkT_n - \frac{\hbar^2}{24m} n \frac{\partial^2}{\partial x_k^2} \log n + O(\hbar^4). \quad (2)$$

We further assume that the fourth order tensor R is specified by the classical form as

$$R = \frac{5}{2} k^2 T_n^2 I, \quad (3)$$

where I is the identity tensor. The quantum potential $\gamma_n = 2b_n \nabla^2 \sqrt{n} / \sqrt{n}$ is derived from $O(\hbar^2)$ corrections to the stress tensor P_{ij} [4]. The external potentials in the current density and the forcing term of carrier heating are corrected by using the quantum potential. Moreover, the quantum corrections to the energy density W are included in the drift contributions to the energy flux S_n and neglected in the diffusive contributions.

We consider only the case of electrons. A four-moments QET model is derived as follows:

$$\varepsilon \Delta \phi = q(n - p - C), \quad (4)$$

$$\frac{1}{q} \operatorname{div} J_n = 0, \quad (5)$$

$$J_n = q \mu_n (\nabla(n \frac{kT_n}{q}) - n \nabla(\phi + \gamma_n)), \quad (6)$$

$$b_n \nabla \cdot (\rho_n \nabla v_n) - \frac{kT_n}{q} \rho_n \nabla v_n = -\frac{\rho_n}{2} (\phi - \phi_n), \quad (7)$$

$$\nabla \cdot S_n = -J_n \cdot \nabla(\phi + \frac{\mu_s}{\mu_n} \gamma_n) - \frac{3}{2} kn \frac{T_n - T_L}{\tau_e}, \quad (8)$$

$$S_n = -\frac{\mu_s}{\mu_n} \left(\frac{5}{2} \frac{kT_n}{q} - \frac{\hbar^2}{24mq} \Delta \log n \right) J_n - \frac{\mu_s}{\mu_n} \frac{5}{2} \left(\frac{k}{q} \right)^2 q \mu_n n T_n \nabla T_n, \quad (9)$$

where $u_n = (\varphi + \gamma_n - \varphi_n)/2$ and $v_n = qu_n/(kT_n)$. φ , φ_n , n , p , and T_n are the electrostatic potential, chemical potential, electron and hole densities, and electron temperature, respectively. ρ_n is the root-density of electrons. ϵ , q , and k are the permittivity of semiconductor, electronic charge, and Boltzmann's constant. C and T_L are the ionized impurity density and the lattice temperature, respectively. $b_n = \hbar^2/(12qm)$, where m and \hbar are an effective mass and Planck's constant. τ_ϵ is the carrier energy relaxation time. μ_n and μ_s are mobility models. For a temperature dependent mobility model, we apply simplified Hänsch's mobility model[7],

$$\frac{\mu(T_n)}{\mu_0} = \left(1 + \frac{3}{2} \frac{\mu_0 k}{q \tau_\epsilon v_s^2} (T_n - T_L)\right)^{-1}, \quad (10)$$

where μ_0 and v_s are low-field mobility and saturation velocity, respectively.

By employing an exponential transformation of variable $\rho_n = \sqrt{n} = \sqrt{n_i} \exp(qu_n/(kT_n))$, the quantum potential equation is replaced by (7) in terms of the variable v_n [10]. If the variable v_n is uniformly bounded, the electron density is maintained to be positive. As mentioned below, this approach provides a numerical advantage for developing the iterative solution method of the QET model as well as the quantum drift diffusion (QDD) model [10].

III. DISCRETIZATION AND ITERATIVE SOLUTION METHOD

Space discretization of the QET model is performed by a new set of unknown variables (φ, v_n, n, T_n) . By employing new variable ξ , the current density J_n and the energy flow S_n can be written in a general form, similar as in the classical ET model [8], [11]. The general flux is introduced as

$$C \left(\nabla \xi - \frac{q}{kT_n} \xi \nabla (\varphi + \gamma_n) \right), \quad (11)$$

where C is constant. $C = q\mu_n$ in J_n and $C = -(5/2)q\mu_s$ in S_n . The variable $\xi = nkT_n/q$ in J_n and $\xi = n(kT_n/q)^2$ in S_n . Using the variable $g = \int (q/(kT_n)) \nabla (\varphi + \gamma_n)$, (11) can be rewritten in the following form as

$$C e^g \nabla (e^{-g} \xi). \quad (12)$$

Using (12), we can apply Scharfetter-Gummel type schemes to (5) and (8) [8], respectively. Space discretization of (7) is performed following our previous work [10], [12] to achieve Scharfetter-Gummel type schemes.

An iterative solution method, which consists of the inner and outer iteration loops, is developed, as shown in Fig.1. It is a critical issue to solve for the unknown ρ_n the quantum potential equation

$$-2b_n \nabla^2 \rho_n + \gamma_n \rho_n = 0. \quad (13)$$

In this case, the iterative solution method requires an additional iteration loop to maintain positive solutions for the root-density of electrons in the inner iteration loop [13]. Hence, in the inner iteration loop, (13) is replaced by (7). The algorithm using the variable v_n in (7) ensures the positivity of the root-density of electrons without introducing damping parameters [10]. We can enhance the robustness of the iterative solution method by introducing a relaxation method with a parameter α , $0 < \alpha < 1$, in the outer iteration loop:

$$T^{m+1} = T^m + \alpha(T_*^{m+1} - T^m). \quad (14)$$

The convergence behavior of electron temperature is shown in Fig.2 as a function of the relaxation parameter. It is clear that the numerical stability is obtained by the relaxation method.

IV. NUMERICAL RESULTS

The numerical results are calculated in a 35nm MOSFET having thin gate oxide thickness of 1.5nm and uniform channel doping of $2.0 \times 10^{18} \text{ cm}^{-3}$. In Fig.3 (a) and (b), we compare the electron density distributions calculated by QDD, QET and classical ET models. The device was biased with $V_g=0.8\text{V}$ and $V_d=0.8\text{V}$. The simulated density distributions are plotted at different positions of the channel. Fig.3 (a) shows the electron density distributions at the source end of the channel. The electron density distributions calculated from the QET and QDD models are almost identical at the source end of the channel. Carrier heating due to the short channel effects results in the spread of electrons towards the bulk in simulations using the QET and ET models. The electron density distributions at the drain end of the channel are shown in Fig.3 (b). The results clearly indicate that the quantum confinement effect is reduced by the enhanced diffusion towards the bulk due to the high electron temperature near the drain. The QET model allows simulations of quantum confinement transport with hot-carrier effects in MOSFETs.

Fig.4 (a), (b), and (c) shows lateral profiles of electron temperature calculated by the QET and ET models in weak inversion and strong inversion regions, and the medium inversion region between the two. The simulations are done at the same drain voltage of 0.8V. As shown in Fig.4 (a), the results in the weak inversion region are almost identical between two models. In Fig.4 (b), we show the results calculated by the QET model at $V_g=0.8\text{V}$ and the ET model at $V_g=0.8\text{V}$ and $V_g=0.5\text{V}$. Fig.4 (c) compares the results in the strong inversion region. At the same gate voltage, the QET model exhibits sharper distributions of electron temperature at the lateral direction, when compared to those calculated by the ET model. These differences are caused by the threshold voltage shift due to the quantum confinement in the channel. In Fig.5, we present the x-component of the current density. The results show that the magnitude of the current density calculated by the QET model at $V_g=0.8\text{V}$ corresponds to that calculated by the ET model at $V_g=0.5\text{V}$ in the medium inversion region. Therefore, the shape of electron temperature distributions is close to that obtained by the ET model at $V_g=0.5\text{V}$, as shown in Fig.4 (b). We observe from Fig.4 (c) a

larger discrepancy of temperature distributions in the strong inversion region due to the strong quantum confinement.

V. CONCLUSION

A four-moments QET model has been derived by using a diffusion scaling in the quantum hydrodynamic model. Numerical methods for the QET model in terms of a new set of variables have been developed. We can enhance the robustness of the iterative solution method by introducing a relaxation method. The QET model allows simulations of quantum confinement transport with hot-carrier effects in scaled MOSFETs. The results reveal the difference of electron temperature distributions between the QET and ET models due to the quantum confinement effects.

ACKNOWLEDGMENT

The authors would like to thank Dr.Shimada for numerical simulations.

REFERENCES

- [1] P.Degond et al., Quantum energy transport and drift diffusion models, *Journal of Statistical Phys.*, vol.118(2005), pp.625-667
- [2] R-C Chen et al., An accelerated monotone iterative method for the quantum-corrected energy transport model, *Journal of Comp. Phys.* vol.204(2005), pp.131-156.
- [3] S. Jin, et al., Simulation of quantum effects in the nano-scale semiconductor device, *Journal of Semi.Tech. and Sci.*, vol.4(2004), pp.32-38.
- [4] M.G.Ancona, and G.J.Iafrate, Quantum correction to the equation of state of an electron gas in a semiconductor, *Phys. Rev. B* 39 (1989), pp. 9536-9540
- [5] C.L.Gardner, The quantum hydrodynamic model for semiconductor devices, *SIAM J.Appl.Math.*, vol.24(1994), pp.409-427
- [6] S-C Lee and T-W Tang, Transport coefficients for a silicon hydrodynamic model extracted from inhomogeneous monte-carlo calculations, *Solid-State Elec.*, vol.35(1992), pp.561-569.
- [7] T.Grasser et al., A review of hydrodynamic and energy-transport models for semiconductor device simulation, *IEEE Proceedings*, vol.91(2003), pp.251-274, 2003.
- [8] M.Gritsch et al., Revision of the standard hydrodynamic transport model for SOI simulation, *IEEE Transactions on Electron Devices*, vol. 49(2002), pp.1814-1820.
- [9] E.Wigner, On the quantum correction for thermodynamic equilibrium, *Phys. Rev.* 40(1932), pp.749-759
- [10] S.Odanaka, Multidimensional discretization of the stationary quantum drift-diffusion model for ultrasmall MOSFET structures, *IEEE Trans. CAD of ICAS*, vol.23(2004), pp.837-842.
- [11] B.Meinerzhagen et al., The influence of the thermal equilibrium approximation on the accuracy of classical two-dimensional numerical modeling of silicon submicrometer MOS transistors, *IEEE Trans. Elec. Devices*, vol.35(1998), pp.689-697.
- [12] S.Odanaka, A high-resolution method for quantum confinement transport simulations in MOSFETs, *IEEE Trans. CAD of ICAS*, vol.26(2007), pp.80-85.
- [13] M.G.de Falco et al., Quantum-corrected drift-diffusion models for transport in semiconductor devices, *Journal of Comp. Phys.* vol.204(2005), pp.533-561

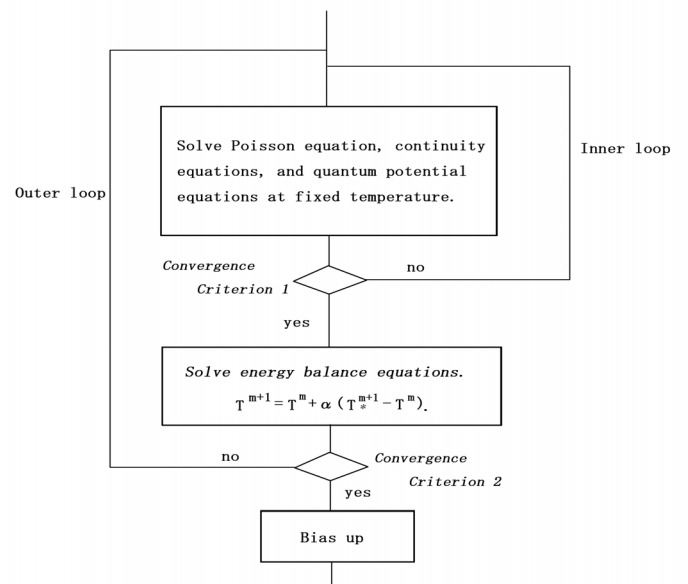


Fig.1 An iterative solution method with a relaxation algorithm

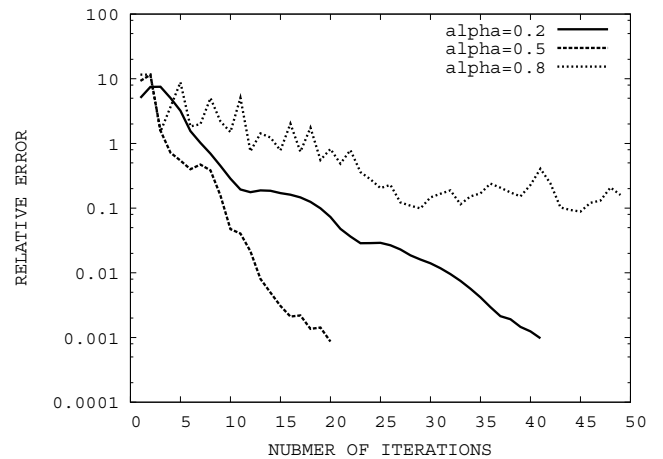
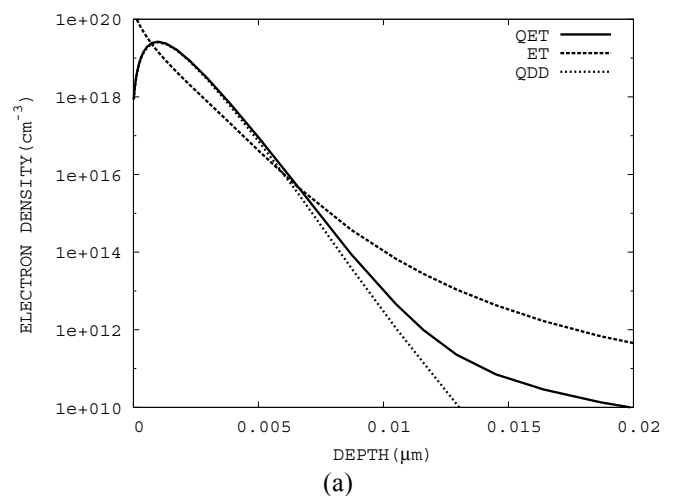


Fig.2 Relative error of electron temperature vs. number of iterations at different relaxation parameters.



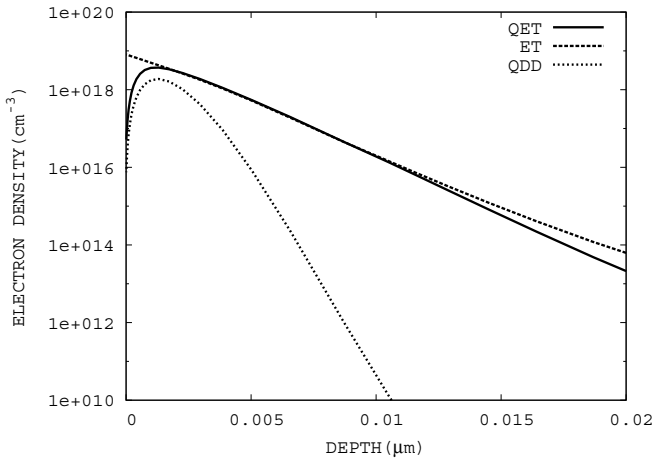


Fig.3 Electron density distributions perpendicular to the interface for a 35nm MOSFET, (a) at the source end of the channel, and (b) at the drain end of the channel. $V_g=0.8V$, $V_d=0.8V$, and $\tau_e = 0.1ps$

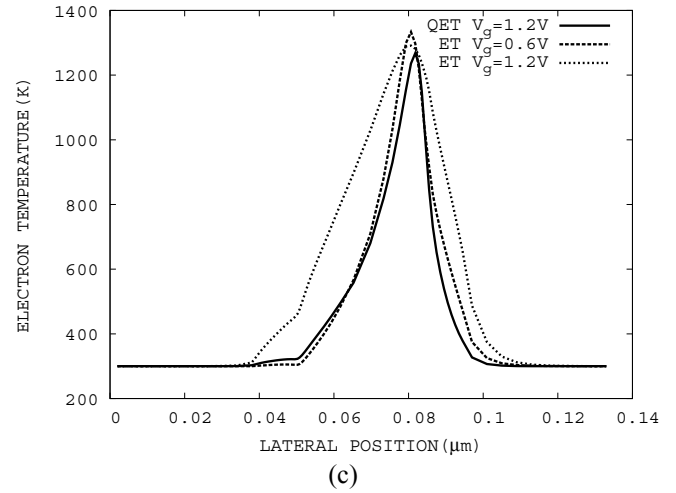


Fig.4 Lateral profiles of electron temperature distributions calculated by QET(solid line) and ET(dotted line) models at the same drain bias of $V_d=0.8V$. (a) QET model at $V_g=0.3V$, ET model at $V_g=0.3V$ and $V_g=0.2V$. (b) QET model at $V_g=0.8V$, ET model at $V_g=0.8V$ and $V_g=0.5V$. (c) QET model at $V_g=1.2V$, ET model at $V_g=1.2V$ and $V_g=0.6V$.

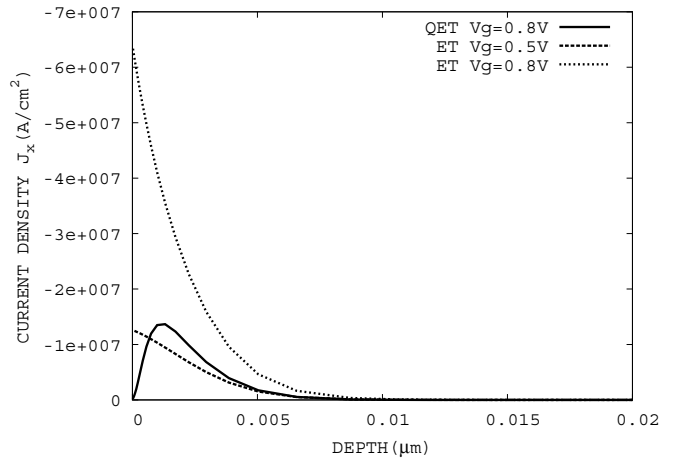
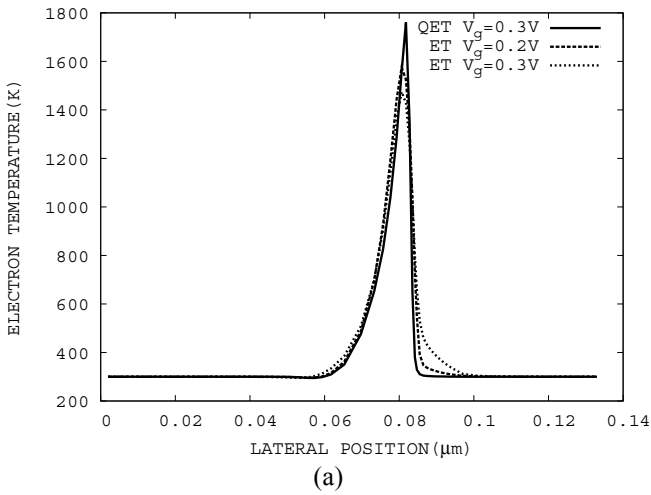


Fig.5 x-Component of current densities perpendicular to the interface for a 35nm MOSFET. QET model at $V_g=0.8V$, ET model at $V_g=0.8V$ and $V_g=0.5V$

